Redox properties of the lipocalin α_1-microglobulin: reduction of cytochrome c, hemoglobin and free iron

Maria Allhorn, Anna Klapyta[§] and Bo Åkerström

Department of Cell and Molecular Biology, Lund University, Lund, Sweden, and

[§]Department of Physical Biochemistry, Jagiellonian University, Krakow, Poland.

Correspondence:

Bo Åkerström, Department of Cell and Molecular Biology, Lund University,

BMC, B14,

221 84 Lund, Sweden

Tel: +46 46-2228578 Fax: +46 46 157756

E-mail: bo.akerstrom@medkem.lu.se

Abstract

α_1-microglobulin (α_1m) is a 26 kDa plasma and tissue glycoprotein. The protein has a heterogeneous yellow-brown chromophore consisting of small unidentified prosthetic groups localized to a free thiol group (C34) and three lysyl residues (K92, K118 and K130) around the entrance to a hydrophobic pocket. It was recently reported that α_1m can bind heme and that a C-terminally processed form of α_1m degrades heme. It is shown here that α_1m has catalytic reductase and NADH-dehydrogenase-like activities. Cytochrome c, nitroblue tetrazolium (NBT), methemoglobin and ferricyanide were reduced by α_1m. Comparison of the reduction rates suggests that methemoglobin is a better substrate than cytochrome c, NBT and ferricyanide. The reactions with cytochrome c and NBT were mediated by superoxide anions since they were inhibited by superoxide dismutase. The addition of the biological electron donors NADH, NADPH or ascorbate enhanced the reduction rate of cytochrome c approximately 30-fold. Recombinant α_1m, which has much less chromophore than plasma and urine α_1m, was a stronger reductant than the latter α_1m-forms. Site-directed mutagenesis of C34, K92, K118 and K130 and thiol group chemistry showed that the C34 thiol group was involved in the redox reaction but relies upon co-operation with the lysyl residues. The redox properties of α_1m may provide a physiological protection mechanism against extracellularly exposed heme-groups and other oxidants.

Keywords: α_1-microglobulin; reductase; electron; superoxide anions; heme; hemoglobin; iron; NAD(P)H; dehydrogenase.

Introduction

The Lipocalins is a protein superfamily with 30-35 members distributed among animals, plants and bacteria [1,2]. The members of the superfamily have a highly conserved three-dimensional structure but very diverse functions. The lipocalin fold consists of eight antiparallel β-strands folded into a barrel with one closed and one open end. The interior of the barrel forms a binding site for small hydrophobic ligands and this structural property is the basis for a surprisingly wide array of biological functions. Retinol-binding protein and prostaglandin D-synthase from mammals, insect bilin-binding protein and plant violaxanthin-de-epoxygenase are examples of lipocalins [3-6].

α_1-microglobulin (α_1m) is one of the originally described lipocalins [7,8] and perhaps also the most widespread member phylogenetically [9,10]. So far, it has been found in mammals, birds, fishes and amphibians. α_1m has a number of intriguing and unusual properties. For example, it has a yellow-brown colour and is charge heterogeneous. This is caused by an array of small chromophore prosthetic groups attached to the amino acid residues C34, K92, K118 and K130, which are localized around the entrance of the lipocalin pocket [11,12]. α_1m is found in blood and in connective tissue in most organs and is most abundant at interfaces between the cells of the body and the environment, such as in lungs, intestine, kidneys and placenta [13-16]. α_1m has immunosuppressive properties, such as inhibition of antigen-induced proliferation of human peripheral lymphocytes, migration and chemotaxis of granulocytes [17,18], IL-2 production by T-cells [19], and activation of the mononuclear cells [20].

Recently, it was shown that α_1m can bind heme/hemin strongly and that a processed form of α_1m (t-α_1m) which is formed by cleavage of the C-terminal tetrapeptide LIPR during incubation with erythrocyte membranes or purified hemoglobin, has heme-degrading properties [21]. In chronic leg ulcers, a hemolytic inflammatory condition where free heme and iron are considered to be pathogenic factors, α_1m was found to bind to heme and co-localized with heme, and t-α_1m was continuously formed [22]. This suggests that α_1m has a role in heme-catabolism and may be part of extracellular protection mechanisms against the deleterious oxidative effects of exposed heme-proteins and heme-groups. Another abundant heme-protein is cytochrome c, a mitochondrial electron-transporter of the respiratory chain. Due to its water-soluble properties, cytochrome c may be exposed to surrounding tissue components during for instance inflammation and other necrotic conditions, and is a potential oxidative threat via its heme-group. Therefore, we investigated the interactions between α_1m and cytochrome c.

Heme, which is linked covalently to cytochrome c, consists of the organic compound protoporphyrin IX chelate-binding an iron-atom. The iron atom acts as an electron acceptor or donor by oscillating between the Fe^{2+} (ferrous) and Fe^{3+} (ferric) oxidation levels. In a neutral buffer, cytochrome c is mainly found in the oxidized Fe^{3+}-form. Here, we show that α_1m reduces cytochrome c to the Fe^{2+}-form, via formation of superoxide anion radicals ($O_2^{\cdot-}$) and using the biological electron donors ascorbate and NADH/NADPH as co-factors. The protein also reduces methemoglobin and free ferric iron, as well as the synthetic electron acceptor nitroblue tetrazolium (NBT). We have investigated the details of this reductase-like property and speculate that it may be part of a heme-degradation mechanism and may constitute a novel antioxidation defence system.

Materials and methods

Recombinant α_1m

Wild-type and mutated variants of α_1m were expressed in *Escherichia coli* (*E.coli*). Using site directed mutagenesis a Cys→Ser substitution was introduced at amino acid position 34 in the C34S-α_1m mutant, and Lys→Thr substitutions at positions 92, 118, 130 in the K(3)T-α_1m mutant. In the recombinant α_1m forms, the N-terminus was elongated by an amino acid sequence containing eight histidines (His-tag) and an enterokinase cleavage site (DDDDKA). The purity of all recombinant α_1m variants was estimated by SDS-PAGE. The results showed distinct protein bands identified as α_1m by Western blotting and N-terminal sequencing. A correct folding of the proteins was confirmed using far UV-circular dichroism spectroscopy (Klapyta et al., manuscript in preparation). The His-tag was removed by incubating 10 mg α_1m with 400 U enterokinase (Sigma Aldrich Sweden AB) for 5 hours at room temperature in 20 mM Tris-HCl, 0.5 M NaCl, pH 8.0. His-tag free α_1m was then separated from enterokinase by gel-chromatography and the N-terminal amino acid sequence determined.

Proteins and reagents

Human α_1m was prepared from plasma [23], urine [24] and baculovirus-infected insect cells [25] as described. T-α_1m was prepared from plasma or recombinant α_1m by incubation with ruptured erythrocytes as described [21]. Mouse monoclonal anti-α_1m, BN11.10, was prepared and purified as described [26] and immobilized to Affi-gel Hz (Bio-Rad Labs, Hercules, CA) at 20 mg/ml following instructions from the merchant. All other proteins were of analytical grade and were purchased from Sigma-Chemicals, St Louis, MO, if not indicated otherwise.

Nitroblue tetrazolium (NBT) was from Boehringer Mannheim GmbH, Mannheim**,** Germany. Reagent solutions were prepared using Millipore-filtrated water. A His_8-tag peptide was synthesised at Chemical Research and Development Laboratory, KJ Ross-Petersen ApS, Holte, Denmark. The purity of the peptide was analysed by HPLC and was estimated to be > 95%.

Reduction of cytochrome c

Bovine heart cytochrome c at the concentrations 6-50 μM was mixed with plasma α_1m, recombinant α_1m or the control proteins ovalbumin and orosomucoid at 5-40 μM. The buffer used in these reactions was either PBS (10 mM sodium phosphate, pH 7.4, 120 mM NaCl, 3 mM KCl) or 20 mM Tris-HCl, pH 7.4, 150 mM NaCl. For pH-studies 20 mM sodium phosphate, 100 mM NaCl at pH 6 and 7 or 20 mM Tris-HCl, 100 mM NaCl at pH 8 and 9, were used. The reduction of cytochrome c was measured as an increase of the absorbance at 550 nm as described below. Where indicated, the reactions were performed with the addition of 3 μM superoxide dismutase, 1 mM KCN or 10 mM NaN_3. In one experiment α_1m was first preincubated with cytochrome c immobilized to CNBr-activated Sepharose ^{TM} 4B at 10 mg protein/ml gel (Amersham Pharmacia Biotech AB, Sweden) at the molar α_1m:cytochrome c ratio 1:15 or only Sepharose, for 5 hours. After centrifugation at 1000 x G for 5 min., the supernatants were analyzed for cytochrome c reduction as described above. Freshly made solutions of N-ethylmaleimide (NEM), NADH, NADPH or ascorbic acid were added to the reaction mixtures at the final concentrations 2-250 μM as indicated.

NADH oxidation

NADH oxidation was followed by measuring the reduction of the absorbance at 340 nm in a mixture containing 10 μM α_1m, 10 μM cytochrome c and 20 μM NADH in 20 mM Tris-HCl,

pH 7.6. The molar concentration of NAD^+ was calculated using the extinction coefficient 6.3 x 10^3 ($M^{-1}cm^{-1}$).

Reduction of nitroblue tetrazolium (NBT)

Measurements of NBT reduction was performed in 10 mM Tris-HCl, pH 8.5, using NBT at 200 μM, α_1m at final concentrations between 1.25 and 10 μM and/or NADH, NADPH or ascorbate at final concentrations of 2-250 μM. In control experiments, KCN or NaN_3 was added to 1 mM or 10 mM final concentration, respectively. The reduction of NBT was measured as an increase of the absorbance at 530 nm as described below.

Methemoglobin reduction

Human methemoglobin, 2.5-50 μM, was incubated at room temperature with 40 μM α_1m or orosomucoid in 20 mM Tris-HCl, 100 mM NaCl pH 7.4. Absorbance at 630 nm was recorded at 1-min intervals and absorbance spectra after 30 minutes.

Ferricyanide reduction

α_1m, 5-40 μM in 20 mM Tris-HCl, pH 7.4, 150 mM NaCl, was incubated with 500 μM potassium ferricyanide ($K_3Fe(CN)_6$) at room temperature for 90 minutes. The amounts of produced ferrocyanide were determined using bathophenanthrolinedisulfonic acid (Sigma-Chemicals) as described by Avron and Shavit [27] by measuring the increase of absorbance at 535 nm and using the reagents as a blank.

Spectrophotometric methods

Kinetic studies were made by recording absorbance values during 20 minutes with 1-minute intervals on a Beckman DU 640i spectrophotometer. Absorbance spectra were measured

using a scan-rate of 1200 nm/min in the UV-VIS region between 250-700 nm. Initial reaction rates, r_i, were calculated from the Δ-absorbance after 5 or 10 minutes and using the extinction coefficients 2.1 x 10^4 $M^{-1}cm^{-1}$ for the cytochrome c $Fe^{3+/2+}$ transition, 1.5 x 10^4 $M^{-1}cm^{-1}$ for the reduction of NBT, and 3.7 x 10^3 $M^{-1}cm^{-1}$ for the reduction of methemoglobin [28].

Electrophoresis

SDS-PAGE was performed using 12% gels in the buffer system described by Laemmli [29] including 2% vol/vol β-mercaptoethanol in the sample buffers. High-molecular-mass standards (Rainbow markers; Amersham Pharmacia Biotech, Uppsala, Sweden) were used.

Analysis of free thiol groups

α_1m was incubated with iodo-[^{14}C]acetamide ([^{14}C]IAA) (Amersham Life Science, specific activity 59.0 mCi (2.2 GBq)/mmol). The reaction mixtures contained 2 μM α_1m in 0.2 M Tris-HCl, pH 8.5, and 1 mM [^{14}C]IAA. The reaction proceeded for 60 minutes at 25°C in the dark. To determine the amounts of bound [^{14}C]IAA, the alkylated α_1m was subjected to SDS-PAGE and phosphoimaging.

Results

Reduction of cytochrome c

The heme group of c-type cytochromes contains iron, which can change from oxidized (Fe^{3+}) to reduced (Fe^{2+}) form. It was observed initially that plasma α_1m and recombinant α_1m (="α_1m") induced a reduction of cytochrome c to the Fe^{2+} form, shown spectrophotometrically in Figure 1 as the appearance of two absorbance peaks at 520 and 550 nm. The reaction was completely inhibited by superoxide-dismutase (SOD), indicating that superoxide anions are involved in the reduction. Recombinant α_1m is equipped with an N-terminal His_8-tag but removal of this (see Materials and Methods) did not decrease the reducing effect, and a synthetic His_8-peptide alone did not reduce cytochrome c. The reduction reaction was not inhibited by the addition of EDTA suggesting that chelatable metal ions are not involved. No inhibition was seen when KCN or NaN_3 was added suggesting a non-heme reaction of α_1m. The concentration of KCN used (1 mM) was shown to have no effect on cytochrome c [30].

The time-dependence of the reduction reaction was followed by reading the absorbance at 550 nm of a 50 μM-solution of cytochrome c and various concentrations of α_1m at regular intervals (Figure 2A). The rate of the reaction increased with increasing α_1m-concentrations and using 40 μM α_1m the rate was initially high but declined slowly, consistent with depletion of the substrate. No reaction was seen when 3 μM SOD was added to cytochrome c with 20 μM α_1m (Figure 2A). The initial reaction rate, r_i, was plotted as a function of the concentration of α_1m (Figure 2B). A faster reaction was observed with recombinant α_1m compared to plasma α_1m (Figure 2B), urine α_1m and recombinant α_1m expressed by insect cells (not shown). A sigmoidal concentration dependence was seen for α_1m, indicating that

the protein act both as a catalyst and substrate in the reaction. Above 10 μM, the rate constant of the reaction was 1.2 x 10^{-4} (s^{-1}) for recombinant α_1m and 0.4 x 10^{-4} (s^{-1}) for plasma α_1m. Orosomucoid, another member of the lipocalin family, did not show any ability to reduce cytochrome c (Figure 2B). The pH-dependence of the reaction, measured at 10 min., is shown in Figure 2C. A several-fold increased reaction rate was observed at pH 8 and 9 compared to pH 6 and 7.

Effect of α_1m variants

The influence of the C34 thiol group of α_1m for the reaction was studied. Figure 3A shows that the C34S-α_1m mutant only had a weak reducing effect on cytochrome c, indicating that the thiol group is involved in the reaction. This was supported by blocking the thiol group with 300 μM N-ethylmaleimide, which resulted in an inhibition of the reduction (Figure 3B). As a control, it was shown that the same concentration of N-ethylmaleimide had no inhibitory effect of the cytochrome c-reduction by 20 μM vitamin C. Human albumin, which also has one free thiol group, did not reduce cytochrome c under these conditions (not shown).

Two other α_1m-variants were studied. The K(3)T-α_1m mutant had a much weaker reducing activity than wildtype α_1m (Figure 3A), showing that the three chromophore-carrying lysyl residues are essential for the reaction even though the C34 thiol group is present (see also below). Finally, t-α_1m, a naturally occurring form of α_1m with heme-degrading properties and lacking the C-terminal tetrapeptide LIPR, reduced cytochrome c much faster than wildtype α_1m, with r_i-values of 2.0 nM/s and 0.32 nm/s, respectively (Figure 3C).

Interaction with NADH, NADPH and ascorbate

NADH strongly enhanced the reduction of cytochrome c by α_1m. Figure 4A shows that 250 μM NADH increased the rate of reduction by 10 μM α_1m almost 30-fold (Table I). 250 μM NADH did not show any reducing activity on its own. These results indicate dehydrogenase properties of α_1m, *i.e.* an electron transfer from NADH to α_1m. Figure 4B shows that the reduction in the presence of NADH was inhibited by SOD, indicating superoxide anions as mediators of the reduction also when NADH is present. A weak remaining activity, however, suggests that a minor superoxide-independent reduction mechanism also may be involved. The C34S- and K(3)T-α_1m mutants displayed a slower reduction of cytochrome c than wildtype α_1m in the presence of NADH (Figure 4C). A stronger accelerating effect of NADH was obtained with K(3)T-α_1m as compared to C34S-α_1m (Table I), suggesting that the C34 thiol, but not K92, K118 and K130 are critical for the interaction with NADH. Interestingly, only weak increases of the reaction rate was seen for t-α_1m in the presence of NADH, suggesting that the tetrapeptide LIPR is essential for the interaction with NADH. Figure 4D shows a rapid initial formation of NAD^+, the oxidized equivalent of NADH, during the NADH-assisted reduction of cytochrome c by α_1m. The NAD^+-production declined, however, after one minute, suggesting that other reaction products become more important at a later stage of the reaction.

Two other biological reductants, NADPH and ascorbate, also strongly accelerated the rate of reduction of cytochrome c by α_1m (Figure 5), indicating that there was no preference for NADH as a reducing co-factor for α_1m. As expected, 50 μM ascorbate alone reacted rapidly with cytochrome c but a synergistic increase of the reaction rate by several factors was observed when when 20 μM α_1m was added (Figure 5B). Table I summarizes the r_i-values for the reactions with and without the reducing cofactors. In general, ascorbate was a better co-

factor than NADH and NADPH, and the C34S-α_1m mutant interacted poorly with all co-factors.

Oxidation of α_1m

To test whether the reduction potential of α_1m was depleted during the reaction with cytochrome c, the protein was exposed for 3 hours to a 15 molar excess of cytochrome c-Sepharose or free Sepharose as a control. After centrifugation, the supernatants containing α_1m were analysed in a new incubation with cytochrome c. As shown in Figure 6, the reaction rate of α_1m incubated with cytochrome c-Sepharose decreased markedly, indicating a depletion, *i.e.* oxidation of α_1m. The reaction rate increased again after addition of NADH, suggesting a regeneration of the reduced form.

The size, charge and redox status of the free thiol group of α_1m during the reactions with cytochrome c and NADH were investigated. No detectable shifts of the mobility of α_1m on SDS-PAGE or non-reducing PAGE were observed (Figure 7A and B). However, an oxidation of the free thiol group by cytochrome c is indicated by the decreased incorporation of [^{14}C]IAA in the presence of cytochrome c (Figure 7C, wt, lane 2). As expected, no labelling of the C34S-α_1m mutant was observed. Interestingly, the thiol group of K(3)T-α_1m was not oxidized by cytochrome c (Figure 7C, K(3)T, lanes 1-2), indicating co-operativity between the C34 thiol group and the K92, K118 and K130 side-chains in the reaction with cytochrome c. Finally, a stronger labelling by [^{14}C]IAA in the presence of NADH, *i.e.* a net reduction of the thiol group, was seen for both wt-α_1m and K(3)T-α_1m (Figure 7C, lanes 3-4), explaining the increased reduction potential in the presence of NADH.

Reduction of NBT, methemoglobin and free iron

The generation of superoxide anions by α_1m was confimed by reduction of NBT. An elevated absorbance at 530 nm, a wavelength specific for reduced NBT, indicated reduction of NBT by recombinant α_1m (Figure 8). The reaction accelerated in a dose-dependent way, a control protein (ovalbumin) was negative (Figure 8A) and the reaction was inhibited to 80% by SOD (Figure 8B). Similar to the reduction of cytochrome c, much less activity was seen with the mutant forms C34S-α_1m and K(3)T-α_1m (Figure 8C), again indicating that the C34, K92, K118 and K130 side-groups are involved in the reaction. The reaction rate was faster with NBT as a substrate ($k = 9 \times 10^{-4}$ s^{-1}) compared to cytochrome c ($k = 1.2 \times 10^{-4}$ s^{-1}). No inhibition of the reaction rates was seen when 1 mM KCN or 10 mM NaN_3 was added, suggesting a non-heme reaction for α_1m.

The oxidized variant of hemoglobin, methemoglobin, was rapidly reduced by α_1m. This was observed as a red-shift of the Soret band (Figure 9A), an increase of absorbance peaks at 560 nm, 577 nm and a decrease of the peak at 630 nm (Figure 9B). The absorbance at 630 nm was plotted as a function of time (Figure 9C) revealing a similar time-frame for this reaction as above. SOD could not inhibit the methemoglobin reduction (Figure 9C) indicating that superoxide anions were not involved in this case. The addition of NADH did not change the reaction rate (not shown).

Ferric cyanide (Fe^{3+}) is a strong artificial electron-acceptor. Figure 10 shows that α_1m has a concentration-dependent reducing effect on ferric cyanide to phenantroline-chelatable ferrous cyanide (Fe^{2+}) which has a specific absorbance peak at 535 nm. The reduction of ferricyanide

by α_1m was not inhibited by SOD, and the addition of NADH did not accelerate the reaction rate (not shown).

The reduction of NBT was also studied in the presence of NADH, NADPH and ascorbate and the initial reaction rates measured (Table I). The reduction of NBT by α_1m was accelerated marginally by ascorbate but not by NADH or NADPH. C34S-α_1m did not reduce NBT even in the presence of the co-factors but K(3)T-α_1m obtained an increased activity by the addition of ascorbate. These results thus support the data obtained with cytochrome c, i.e. that the C34 thiol but not K92, K118 and K130 is critical for the interaction with the co-factors. NADH, NADPH and ascorbate alone reacted strongly with ferricyanide and methemoglobin, preventing interpretation of the results. Taken together, the data in Table I suggests that methemoglobin is a better substrate for the α_1m-reductase activity and ascorbate the preferred electron-donating cofactor.

Discussion

The present report shows that the plasma and tissue protein α_1m has cytochrome c-, methemoglobin- and ferri-reductase activity, and that the reaction with cytochrome c is enhanced by NADH, NADPH and ascorbate. A possible reaction scheme which explains the results and depicts α_1m as a NADH-dehydrogenase:cytochrome c-reductase is shown in Figure 11A. According to this model, an oxidized form of α_1m (α_1m^+) is formed by the reduction of O_2, methemoglobin or Fe^{3+}. The superoxide anion radical, O_2^-, which is formed by reduction of O_2, subsequently reduces cytochrome c or NBT. The oxidized α_1m^+ is reduced again by NADH, NADPH or ascorbate, regenerating α_1m and thereby accelerating the reduction rates.

Figure 11B illustrates a tentative reaction mechanism for the reduction reactions. The results strongly indicate that the only free thiol group of α_1m is part of the active site for the reduction reaction. The reaction with cytochrome c leads to oxidation of the thiol, and blocking of the group with N-ethylmaleimide or changing Cys34 to Ser by site-directed mutagenesis inhibits the reaction. The three-dimensional structure of α_1m is not yet known, but modelling studies based on published lipocalin structures shows that the Cys34 residue is most likely located on a solvent-exposed flexible loop lining the opening of the lipocalin pocket [31]. This is consistent with the promiscuous reaction pattern observed (α_1m can interact with many substrates and cofactors). No oxidation of the thiol group of the K(3)T-α_1m mutant was observed, implicating the Lys residues in positions 92, 118 and 130 as involved in the reaction, perhaps by creating an electronegative environment around the thiol group or by an electron transfer from the Lys residues to the Cys34 thiol (Figure 11B). The three-dimensional model of α_1m shows that Lys 92, 118 and 130 are also located close to the

rim of the lipocalin pocket and it may thus be possible for Cys 34 to interact both with the Lys-groups and the electron-accepting substrates. In urine α_1m the three Lys residues carry chromophore prosthetic groups [12] and the Cys34 thiol group is partially oxidized in a non-reducable manner [32]. In contrast, only very small amounts of chromophores are seen in recombinant α_1m. The lower reductase activity of urine and plasma α_1m may therefore be explained by irreversible blocking of these four residues.

The rate of the reduction reaction was amplified approximately thirty-fold by the electron donors NADH, NADPH and ascorbate. As illustrated in Figure 11A, these compounds may act by regenerating α_1m, allowing a new cytochrome c reduction cycle to take place. This model of the catalytic mechanism is supported by several findings: (1) NADH can regenerate the reduction potential of α_1m after reaction with an excess of cytochrome c-Sepharose; (2) NADH accelerates the reduction reaction in a concentration-dependent manner and (3) NADH can reduce the thiol group of α_1m. The acceleration factor by NADH was approximately the same for wildtype α_1m and the K(3)T-mutant, suggesting that the Lys residues are not involved in the interaction with NADH.

It is doubtful whether NADH or NADPH can act as co-factors of α_1m in vivo. The protein is mainly found in plasma and extracellular tissue fluids [13,14,33] and is therefore co-distributed with ascorbate rather than NADH and NADPH. Ascorbate also gave the highest acceleration factor for the reaction with cytochrome c and NBT (Table 1) and the combination of α_1m and ascorbate yielded a much stronger reaction than ascorbate's own reaction with cytochrome c (Figure 5B). Interestingly, glutathione also accelerated the reduction reaction of α_1m with cytochrome c and NBT (not shown) and our results suggest that α_1m can interact

with a wide spectrum of different biological electron donors rather than being specific for a particular co-factor.

The truncated form of α_1m, t-α_1m, showed a faster reduction rate than full-length α_1m. T-α_1m is formed by incubation with hemoglobin or erythrocyte membranes and involves processing of the C-terminal tetrapeptide LIPR [21]. This suggests that the reduction reaction of α_1m is regulated by the C-terminal tetrapeptide LIPR and that t-α_1m may be an activated form of the reductase. T-α_1m was previously shown to bind and degrade heme and an alternative explanation is that the increased reducing potential of t-α_1m is a result of degradation products of heme, for example bilirubin, associated with the protein. T-α_1m indeed shows an absorbance spectrum consistent with binding of bilirubin [21]. Bilirubin has anti-oxidant properties partly due to its oxidation to biliverdin [34] and may therefore act as an electron donor to cytochrome c directly or using α_1m as an intermediate, explaining the increased reducing properties of t-α_1m. Addition of heme to full-length α_1m yields an α_1m-heme complex [21] which has weaker reducing properties compared to α_1m alone (not shown), arguing against α_1m-bound heme as an explanation for the effects.

There are several functional implications of the reductase activity of α_1m. (1) A biological consequence of the reducing properties is anti-oxidation, i.e. α_1m may either reduce biological oxidants such as cytochrome c, methemoglobin and ferric iron in vivo and thereby prevent them from exerting oxidative stress on tissue components, and/or repair the oxidized target molecules by re-reducing them. (2) The reduction of ferric iron may be important for the uptake of iron in the gut or sequestering of iron by cellular ferritin. In both these cases the iron should be in its reduced form. α_1m is present in the intestinal epithelium, enriched at the tips of the microvilli [16, 33] underscoring the former possibility. (3) The reducing activity of

t-α_1m may be part of a heme degradation mechanism. As mentioned above, t-α_1m can degrade heme, possibly forming bilirubin. Heme oxygenase is an intracellular enzyme [35] that catalyzes the degradation of heme to bilirubin, CO and free iron. The reaction, which includes several reduction steps, is assisted by NADPH:cytochrome P450 reductase and NAD(P)H:biliverdin reductase [36]. In a tentative heme degradation reaction, α_1m may be its own reductase. (4) The reductase activity could provide an explanation for the immunosuppressive properties of α_1m. Antigen-induced activation of leukocytes exploits signalling pathways which are also activated by ROS and other pro-oxidants [37,38]. The inhibition of antigen-induced proliferation and IL-2 production of lymphocytes, migration of neutrophils, IL-1-production and oxidative burst of monocytes, which has been reported for α_1m, may therefore be an indirect result of a general reduction of pro-oxidant levels around the cells.

In conclusion, the unexpected reductase and dehydrogenase properties of α_1m described in this paper may provide a mechanistic explanation for the previously suggested functions of α_1m as a heme-scavenger and immunosuppressor, and leads to the proposal of a novel function as a physiological anti-oxidant.

Table 1. Initial reaction rates of the reduction of cytochrome c, NBT and methemoglobin by various forms of α_1m with or without NADH, NADPH or ascorbate.

	r_i [a] (nM/s)			
	-	NADH	NADPH	ascorbate
Cytochrome c				
α_1m	0.32 (1.8) [b]	9.0	8.0	12.0
C34S-α_1m	0.21 (0.10) [b]	1.0	<0.05	<0.05
K(3)T-α_1m	0.16 (0.26) [b]	5.0	<0.05	11.7
NBT				
α_1m	5.0	3.0	4.0	7.0
C34S-α_1m	0.4	<0.05	<0.05	0.2
K(3)T-α_1m	4.0	0.3	2.0	23.0
Methemoglobin [c]				
α_1m	24			
C34S-α_1m	15			
K(3)T-α_1m	21			
Ferricyanide [c]				
α_1m	6			
C34S-α_1m	3			
K(3)T-α_1m	6			

[a] Cytochrome c (50 μM), NBT (200 μM), methemoglobin (50 μM) or ferricyanide (50 μM) and α_1m (10 μM) were mixed with buffer (-) or NADH (50 μM), NADPH (50 μM) or ascorbate (50 μM). The initial reaction rates were calculated from the net absorbance increase at 550 nm after 5 min for cytochrome c, 530 nm for NBT and the net decrease at 630 nm for methemoglobin.

[b] The rate of the reduction of cytochrome c without NADH, NADPH or ascorbate was also measured using 20 μM α_1m.

[c] The effects of NADH, NADPH and ascorbate on the reactions with methemoglobin and ferricyanide are not included because of the high background activities of NADH, NADPH and ascorbate on these electron acceptors.

Figure legends

Figure 1.

Reduction of cytochrome c by α_1m. Absorbance spectra of 6 μM cytochrome c in PBS, incubated for 3 h with 10 μM α_1m (recombinant), 10 μM plasma α_1m, 10 μM α_1m + 3 μM SOD or buffer. The reagents without cytochrome c were used as blanks.

Figure 2.

Characterization of the reduction of cytochrome c by α_1m. (A) Time-dependence. The absorbance at 550 nm of 50 μM cytochrome c and various concentrations of α_1m, or 50 μM cytochrome c, 20 μM α_1m and 3 μM SOD, was read at 1-min intervals. (B) Concentration dependence. The initial reaction rates (r_i) were calculated from the net absorbance increase after ten minutes of 50 μM cytochrome c plus various concentrations of α_1m, plasma α_1m and orosomucoid, and plotted as a function of the α_1m concentration. (C) pH-dependence. The net absorbance increase at 550 nm of mixture of cytochrome c (50 μM) and α_1m (40 μM) was read after five minutes at pH 6, 7, 8 and 9. Each point shows the mean of triplicates and SEM.

Figure 3.

Reduction of cytochrome c by different α_1m-forms. (A) The initial rates (r_i) were calculated from the net absorbance increase at 550 nm after five minutes for 50 μM cytochrome c plus various concentrations of α_1m, C34S-α_1m or K(3)T-α_1m, and plotted as a function of the α_1m concentration. Each point shows the mean of triplicates and SEM. (B) The absorbance at 550 nm of 50 μM cytochrome c and 20 μM α_1m, with or without 300 μM N-ethylmaleimide, was read at 1-min intervals. (C) The absorbance at 550 nm of 50 μM

cytochrome c and 20 μM α_1m or 20 μM t-α_1m was read at 1-min intervals. Each point shows the mean of triplicates and SEM.

Figure 4.

Acceleration of cytochrome c-reduction with NADH. (A) The absorbance at 550 nm of 20 μM cytochrome c, 10 μM α_1m, and NADH at various concentrations was read at 5-min intervals. (B) The absorbance at 550 nm of 50 μM cytochrome c, 10 μM α_1m and 50 μM NADH, with or without 1.5 μM SOD, was read at 1-min intervals. (C) The absorbance at 550 nm of 50 μM cytochrome c, 10 μM α_1m, C34S-α_1m or K(3)T-α_1m and 50 μM NADH was read at 1-min intervals. (D) NAD^+ was measured in a mixture of 10 μM α_1m, 10 μM cytochrome c and 20 μM NADH by reading the absorbance at 340 nm at 15-sec intervals.

Figure 5.

Acceleration of cytochrome c-reduction with NADPH and ascorbate. (A) The absorbance at 550 nm of 50 μM cytochrome c and 50 μM NADPH alone ("-α_1m") or with the addition of 5 μM α_1m ("+α_1m"), was read at 1-min intervals. (B) The absorbance at 550 nm of 50 μM cytochrome c and 50 μM ascorbate alone ("-α_1m") or with the addition of 20 μM α_1m ("+α_1m"), was read at 1-min intervals. Each point shows the mean of triplicates and SEM.

Figure 6.

Depletion of reducing potential of α_1m. α_1m (80 μM) was pre-incubated with 1.2 mM cytochrome c-Sepharose for five hours and centrifuged. The supernatant was then diluted to the final α_1m-concentration of 40 μM and incubated with 50 μM soluble cytochrome c (●) or cytochrome c and 250 μM NADH (■). As a control, α_1m was pre-incubated with

unconjugated Sepharose for five hours, centrifuged and then incubated with soluble cytochrome c (▼). The absorbance at 550 nm of the solutions were read at different time points.

Figure 7.

Electrophoresis and thiol group-labelling of α_1m. (A) SDS-PAGE with 2-mercaptoethanol or (B) non-denaturing PAGE of α_1m (lane 1), α_1m + cytochrome c (lane 2), α_1m, cytochrome c + NADH (lane 3) or α_1m + NADH (lane 4). Ten µl of the samples were applied and the concentrations were 10 µM (α_1m), 10 µM (cytochrome c) and 50 µM (NADH). The gels were stained with Coomassie Brilliant Blue. (C) SDS-PAGE with 2-mercaptoethanol of 10 µl 2 µM α_1m, C34S-α_1m or K(3)T-α_1m, incubated with buffer (lane 1), 2 µM cytochrome c (lane 2), 2 µM cytochrome c + 5 µM NADH (lane 3), or 5 µM NADH (lane 4). [^{14}C]IAA was added to 1 mM and the samples were separated by SDS-PAGE, stained and analyzed by phosphoimaging.

Figure 8.

Reduction of NBT by α_1m. (A) The absorbance at 530 nm of 200 µM NBT and various concentrations of α_1m, or ovalbumin at 10 µM was read at 1-min intervals. (B) The absorbance at 530 nm of 200 µM NBT and 5 µM α_1m, with or without 1.5 µM SOD, was read at 1-min intervals. (C) The initial reaction rates (r_i) were calculated from the net absorbance increase after five minutes for 200 µM NBT plus various concentrations of α_1m, C34S-α_1m or K(3)T-α_1m and plotted as a function of the α_1m concentration. Each point shows the mean of triplicates and SEM.

Figure 9.

Reduction of methemoglobin by α_1m. Human methemoglobin (A: 2.5 μM, B: 25 μM, C: 50 μM) was mixed with 40 μM α_1m, C34S-α_1m, K(3)-α_1m, 40 μM α_1m + 3 μM SOD or 40 μM orosomucoid. (A and B) Absorbance spectra were read after 30 minutes. (C) Δ-absorbance at 630 nm was read at 1-min intervals.

Figure 10.

Reduction of ferricyanide by α_1m. Ferricyanide ($K_3Fe^{3+}(CN)_6$), 500 μM, was incubated with various concentrations of α_1m for 90 minutes. The production of ferrous iron (Fe^{2+}) was determined by the phenantroline method. Each point shows the mean of triplicates and SEM.

Figure 11.

Tentative reaction mechanism of α_1m. (A) α_1m reduces cytochrome c and NBT via formation of superoxide (the reaction is SOD-inhibitable). The superoxide is hypothetically formed by reduction of molecular oxygen. α_1m also reduces methemoglobin and ferric iron directly (this reaction is not SOD-inhibitable). The oxidized α_1m (α_1m^+), formed by the reduction, is reduced again by NADH, NADPH and ascorbate. These compounds consequently accelerate the reactions. (B) The active site of α_1m is constituted by the thiol group of the unpaired cysteine in position 34, and Lys 92, 118 and 130. These four side-chains are co-located at the opening of the lipocalin pocket. The thiol group, as a result of co-operation with the lysyl groups, donates an electron to the substrate and becomes oxidized.

Abbreviations

α_1m	α_1-microglobulin
C34S-α_1m	α_1-microglobulin mutated at amino acid position 34
K(3)T-α_1m	α_1-microglobulin mutated at amino acid positions 92, 118 and 130
t-α_1m	truncated α_1-microglobulin without C-terminal tetrapeptide LIPR
EDTA	ethylenediamineteraacetic acid
[^{14}C]IAA	iodo-[^{14}C]acetamide
LIPR	leucine-isoleucine-proline-arginin
NADH	nicotinamide adenine dinucleotide
NAD^+	oxidized NADH
NADPH	nicotinamide adenine dinucleotide phosphate
NBT	nitroblue tetrazolium
NEM	N-ethylmaleimide
PBS	phosphate buffer saline
r_i	initial reaction rate
ROS	reactive oxygen species
SDS-PAGE	sodium dodecyl sulfate-polyacrylamide gel electrophoresis
SEM	standard error of mean
SOD	superoxide dismutase

REFERENCES

Okado-Matsumoto, A.; Fridovich, I: Assay of superoxide dismutase: Cautions relevant to use of cytochrome c, a sulfonated tetrazolium, and cyanide. Anal. Biochem. 298: 337-342; 2001.

[1] Flower, D. R. The lipocalin protein family: structure and function. *Biochem. J.* **318:**1-14; 1996.

[2] Åkerström, B.; Flower, D.; and Salier, J. P. Lipocalins: Unity in Diversity. *Biochim. Biophys. Acta.* **1482:**1-8; 2000.

[3] Newcomer, M.; Ong, D. Plasma retinol-binding protein: structure and function of the prototypic lipocalin. *Biochim. Biophys. Acta.* **1482:**57-64; 2000.

[4] Urade, Y.; Hayaishi, O. Biochemical, structural, genetic, physiological and patophysiological features of lipocalin-type prostaglandin D-synthase. *Biochim. Biophys Acta.* **1482:**259-271; 2000.

[5] Huber, R.; Schneider, M.; Mayr, I.; Muller, R.; Deutzmann, R.; Suter, F.; Zuber, H.; Falk, H.; Kayser, H. Molecular structure of the bilin binding-protein (BBP) from *Pieris brassicae* after refinement at 2.0-Å resolution. *J. Mol. Biol.* **198:**499-513; 1987.

[6] Hieber, AD.; Bugos R. C.; Yamamoto, H. Y. Plant lipocalins: violaxanthin de-epoxidase and zeaxanthin epoxidase. *Biochim. Biophys. Acta.* **1482:**84-91; 2000.

[7] Ekström, B.; Peterson, P. A.; Berggård, I. A urinary and plasma α_1-glycoprotein of low molecular weight: isolation and some properties. *Biochem. Biophys. Res. Com.* **65:**1427-1433; 1975.

[8] Pervaiz, S.; Brew, K. Homology of beta-lactoglobulin, serum retinol-binding protein, and protein HC. *Science* **228:**335-7; 1985.

[9] Åkerström, B.; Lögdberg, L. An intriguing member of the lipocalin protein family: α_1-microglobulin. *Trends Biochem. Sci.* **15:**240-243; 1990.

[10] Åkerström, B.; Lögdberg, L.; Berggård, T.; Osmark, P.; Lindqvist, A. α_1-microglobulin – a yellow-brown lipocalin. *Biochim. Biophys. Acta.* **1482:**172-184; 2000.

[11] Escribano, J.; Grubb, A.; Calero, M.; Méndez, E. The protein HC chromophore is linked to the cysteine residue at position 34 of the polypeptide chain by a reduction-resistant bond and causes the charge heterogeneity of protein HC. *J. Biol. Chem.* **266:**15758-15763; 1991.

[12] Berggård, T.; Cohen, A.; Persson, P.; Lindqvist, A.; Cedervall, T.; Silow, M.; Thøgersen, I. B.; Jönsson, J. Å.; Enghild, J. J.; Åkerström, B. α_1-microglobulin chromophores are located to three lysine residues semiburied in the lipocalin pocket and associated with a novel lipophilic compound. *Prot. Sci.* **8:**2611-2620; 1999.

[13] Ødum, L.; Nielsen, H. W. Human protein HC (α_1-microglobulin) and inter-alpha-trypsin inhibitor in connective tissue. *Histochem. J.* **26:**799-803; 1994.

[14] Berggård, T.; Oury, T. D.; Thørgersen, I. B.; Åkerström, B.; Enghild, J. J. α_1-microglobulin is found both in blood and in most tissues. *J. Histochem. Cytochem.* **46:**887-893; 1998.

[15] Berggård, T.; Enghild, J. J.; Badve, S.; Salafia, C. M.; Lögdberg, L.; Åkerström, B. Histologic distribution and biochemical properties of α_1-microglobulin in human placenta. *Am. J. Reprod. Immunol.* **41:**52-60; 1999.

[16] Lögdberg, L.; Åkerström, B.; Badve, S. Tissue distribution of the lipocalin α_1-microglobulin in the developing human fetus. *J. Histochem. Cytochem.* **48:**1545-1552; 2000.

[17] Lögdberg, L.; Åkerström, B. Immunosupressive properties of α_1-microglobulin. *Scand. J. Immunol.* **13:**383-390; 1981.

[18] Méndez, E.; Fernández-Luna, J. L.; Grubb, A.; Leyva-Cobián, F. Human protein HC and its IgA complex are inhibitors of neutrophil chemotaxis. *Proc. Natl. Sci.* **88:** 1472-1475; 1986.

[19] Wester, L.; Michaelsson, E.; Holmdahl, R.; Olofsson, T.; Åkerström, B. Receptor for alpha1-microglobulin on lymphocytes: inhibition of antigen-induced interleukin-2 production. *Scand. J. Immunol.* **48:**1-7; 1998.

[20] Santin, M.; Cannas, M. Collagen-bound α_1-microglobulin in normal and healed tissues and its effect on immunocompetent cells. *Scan. J. Immunol.* **50:**289-295; 1999.

[21] Allhorn, M.; Berggård, T.; Nordberg, J.; Olsson, M. L.; Åkerström, B. Processing of the lipocalin α_1-microglobulin by hemoglobin induces heme-binding and heme-degradation properties. *Blood.* **99:**1894-1901; 2002.

[22] Allhorn, M.; Lundqvist, K.; Schmidtchen, A.; Åkerström, B. Heme-scavenging role of α_1-microglobulin in chronic ulcers. *J. Invest. Dermat*. **121:**640-646; 2003.

[23] Berggård, T.; Thelin, N.; Falkenberg, C., Enghild, J. J.; Åkerström, B. Prothrombin, albumin and immunoglobulin A form covalent complexes with α_1-microglobulin in human plasma. *Eur. J. Biochem.* **245:**676-683; 1997.

[24] Åkerström, B.; Bratt, T., Enghild, J. J. Formation of the α_1-microglobulin chromophore in mammalian and insect cells: a novel post-translational mechanism? *FEBS Lett.* **362:**50-54; 1995.

[25] Wester, L.; Johansson, M. U.; Åkerström, B. Physicochemical and biochemical characterisation of human α_1-microglobulin expressed in baculovirus-infected insect cells. *Protein Expr. Purif.* **11:**95-103; 1997.

[26] Babiker-Mohamed, H.; Olsson, M. L.; Winquist, O.; Nilsson, B. H. K.; Lögdberg, L.; Åkerström, B. Characterisation of monoclonal anti-α_1–microglobulin antibodies:

Binding strength, binding sites, and inhibition of antigen-induced lymphocyte stimulation. *Scand. J. Immunol.* **34:**655-666; 1991.

[27] Avron, M.; Shavitt, N. A sensitive and simple method for determination of ferrocyanide. *Anal. Biochem.* **6:**549-554; 1963.

[28] Halliwell, B.; Gutteridge, J. M. C. *Free radicals in biology and medicine*. New York: Oxford University Press Inc. 1999.

[29] Laemmli, U. K. Cleavage of structural proteins during the assembly of the head of bacteriophage T4. *Nature.* **227:**680-685; 1970.

[30] Okado-Matsumoto, A., Fridovich, I. Assay of superoxide dismutase: Cautions relevant to use of cytochrome c, a sulfonated tetrazolium, and cyanide. *Anal. Biochem*. **298**: 337-342; 2001.

[31] Villoutreix, B.; Åkerström, B.; Lindqvist, A. Structural model of human α_1-microglobulin: proposed scheme for the interaction with protein C. *Blood Coagul. Fibrinol.* **11:**261-275; 2000.

[32] Ekström, B.; Berggård, I. Human α_1-microglobulin. Purification procedure, chemical and physicochemical properties. *J. Biol. Chem.* **252:**8048-8057; 1977.

[33] Larsson, J.; Wingårdh, K.; Davies, J. R.; Lögdberg, L.; Strand, S. E.; Åkerström, B. Distribution of ^{125}I-labelled α_1-microglobulin in rats after intravenous injection. *J. Lab. Clin. Med.* **137:**165-175; 2001.

[34] Baranano, D. E.; Rao, M.; Ferris, C. D.; Snyder, S. H. Biliverdin reductase: a major physiologic cytoprotectant. *Proc. Natl. Acad. Sci.* **99:**16093-16098; 2002.

[35] Tenhunen, R.; Marver, R. S.; Schmid, J. Microsomal heme oxygenase: characterization of the enzyme. *J. Biol. Chem.* **244:**6388-6394; 1969.

[36] Ryter, S. W.; Tyrrell, R. M. The heme synthesis and degradation pathways: role in oxidant sensitivity. Heme oxygenase has both pro- and antioxidant properties. *Free Radic Biol Med.* **28:**289-309; 2000.

[37] Matsue, H.; Edelbaum, D.; Shalhevet, D.; Mizumoto, N.; Yang, C.; Mummert, M. E.; Oeda, J.; Masayasu, H.; Takashima, A. Generation and function of reactive oxygen species in dendritic cells during antigen presentation. *J. Imunol.* **171:**3010-8; 2003.

[38] Reth, M. Hydrogen peroxide as second messenger in lymphocyte activation. *Nature Immunol.* **3**:1129-1134; 2002.

Figure 1

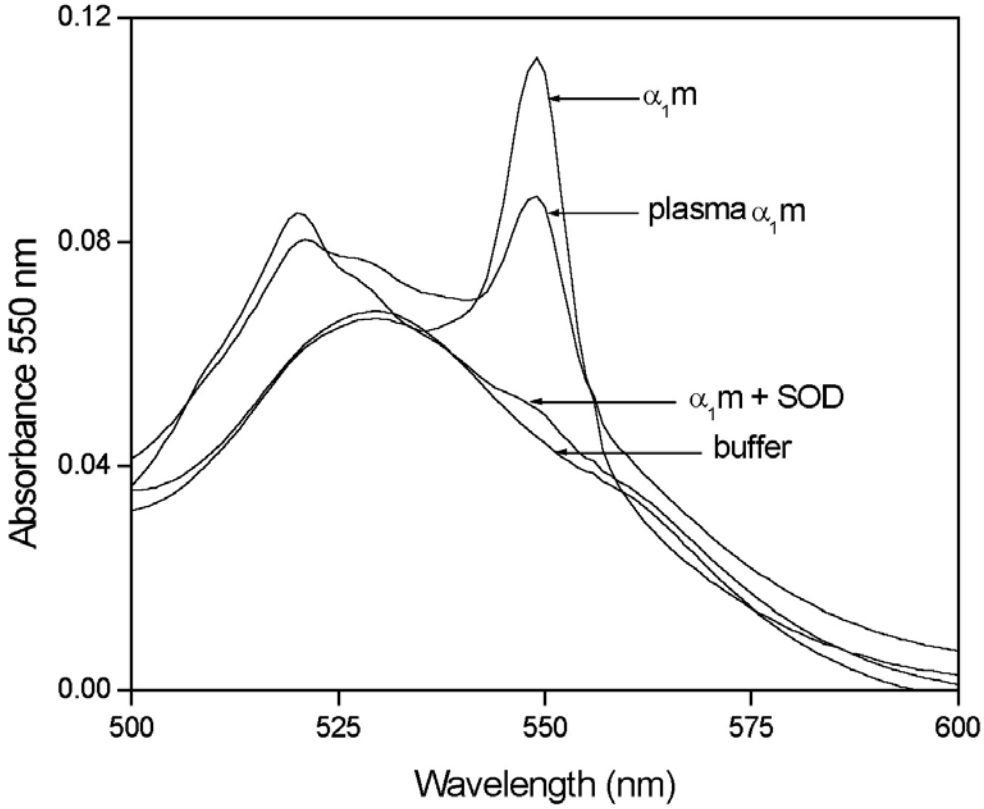
0.12
0.08
0.04
0.00
Absorbance 550 nm
500
525
550
575
600
Wavelength (nm)
α1m
plasma α1m
α1m + SOD
buffer

Figure 2

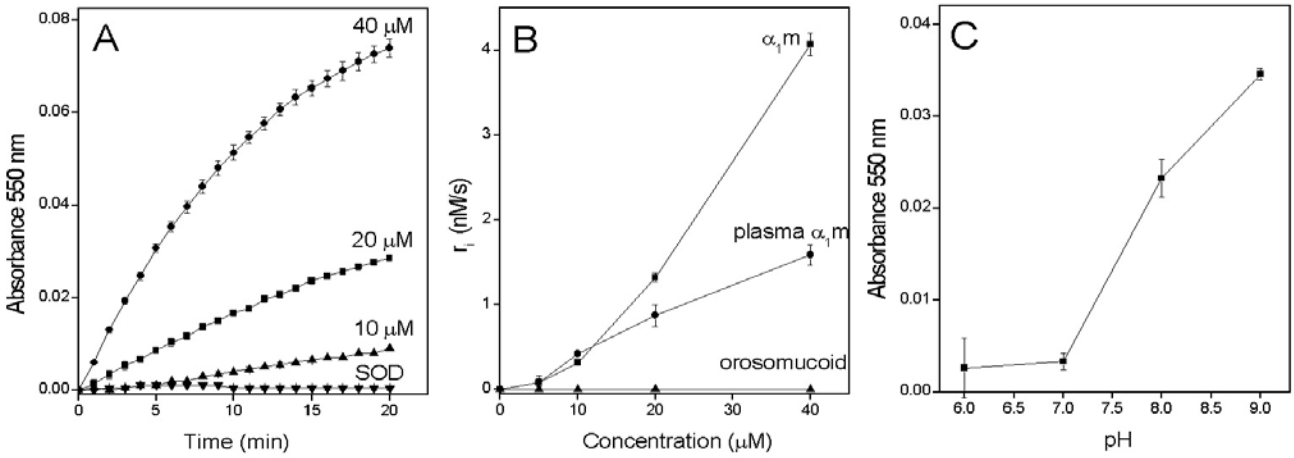
A
40 μM
20 μM
10 μM
SOD
Absorbance 550 nm
Time (min)
B
α1m
plasma α1m
orosomucoid
ri (nM/s)
Concentration (μM)
C
Absorbance 550 nm
pH

Figure 3

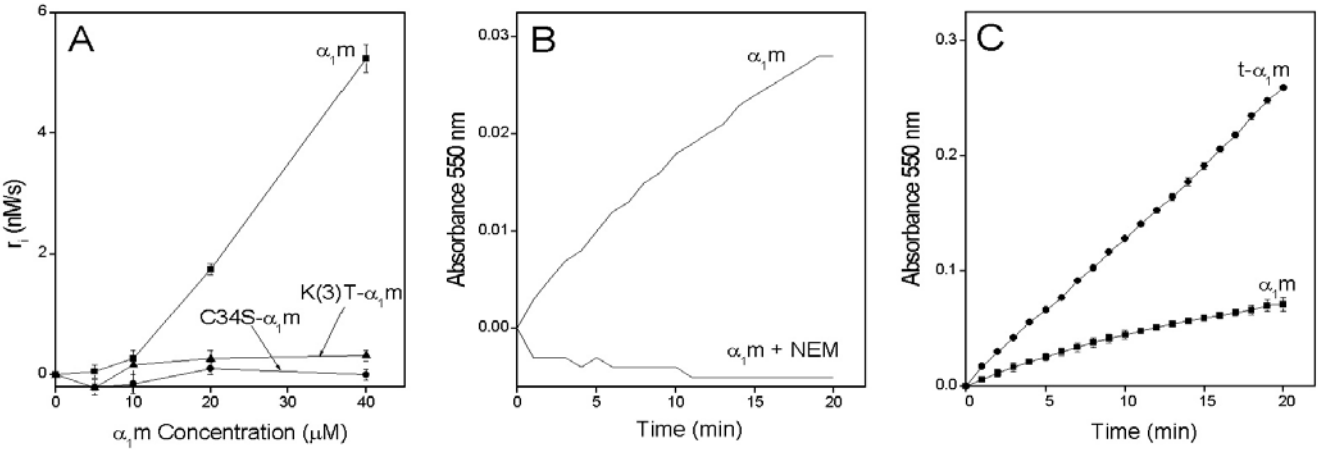
A
α_1m
K(3)T-α_1m
C34S-α_1m
r_i (nM/s)
α_1m Concentration (μM)
B
α_1m
α_1m + NEM
Absorbance 550 nm
Time (min)
C
t-α_1m
α_1m
Absorbance 550 nm
Time (min)

Figure 4

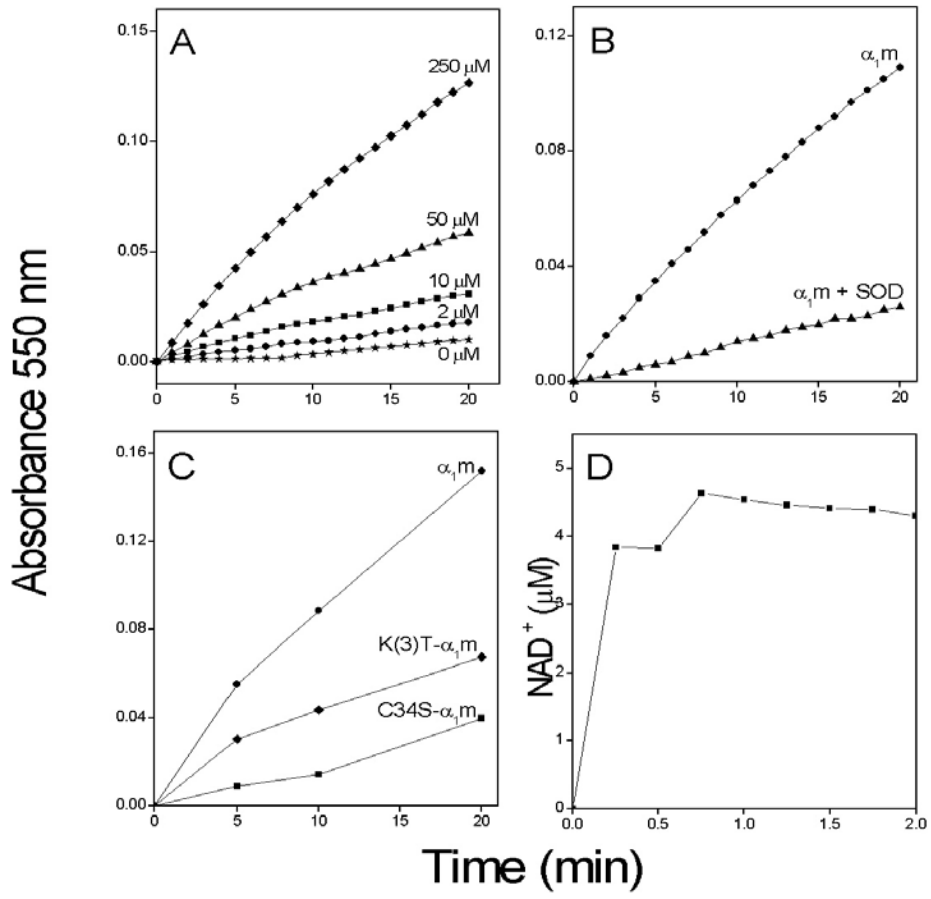
A
250 μM
50 μM
10 μM
2 μM
0 μM
B
α1m
α1m + SOD
C
α1m
K(3)T-α1m
C34S-α1m
D
NAD+ (μM)
Absorbance 550 nm
Time (min)

Figure 5

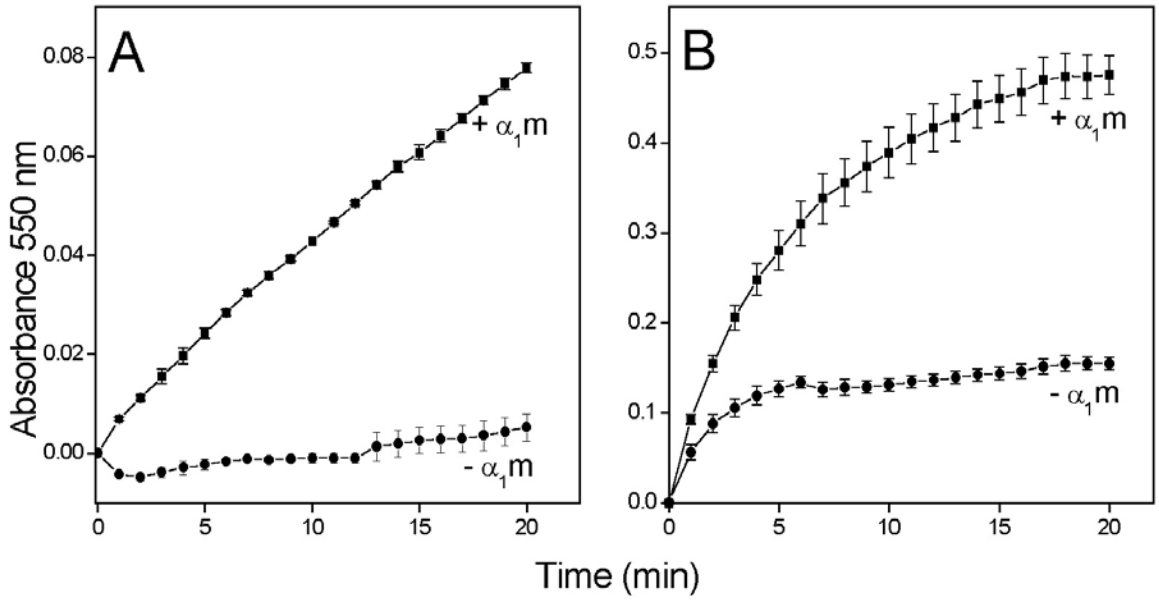
A
B
+ α1m
- α1m
Absorbance 550 nm
Time (min)
0.08
0.06
0.04
0.02
0.00
0.5
0.4
0.3
0.2
0.1
0.0
0
5
10
15
20

Figure 6

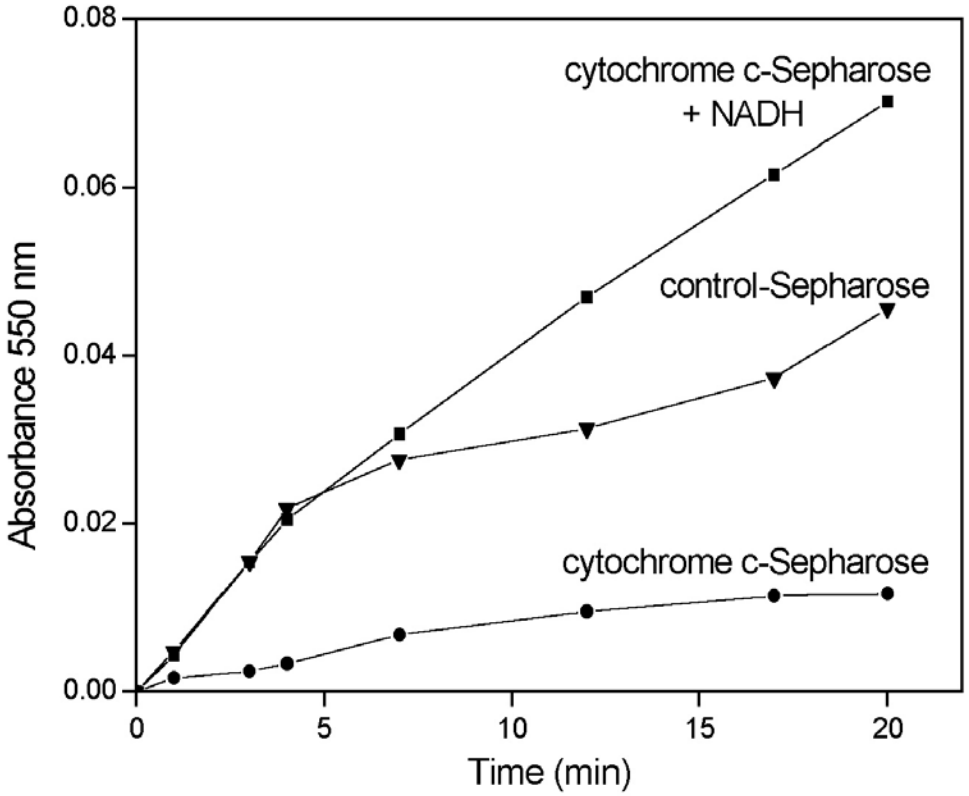
0.08
0.06
0.04
0.02
0.00
Absorbance 550 nm
0
5
10
15
20
Time (min)
cytochrome c-Sepharose
+ NADH
control-Sepharose
cytochrome c-Sepharose

Figure 7

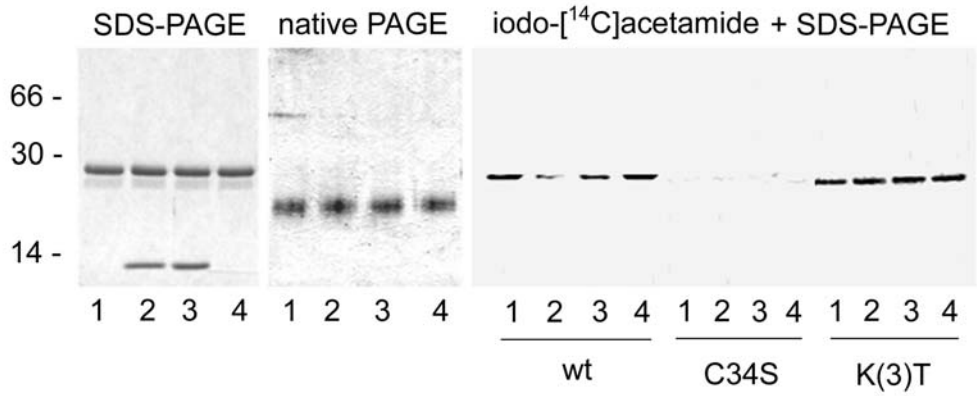
SDS-PAGE
native PAGE
iodo-[14C]acetamide + SDS-PAGE
66 -
30 -
14 -
1 2 3 4 1 2 3 4
1 2 3 4 1 2 3 4 1 2 3 4
wt
C34S
K(3)T

Figure 8

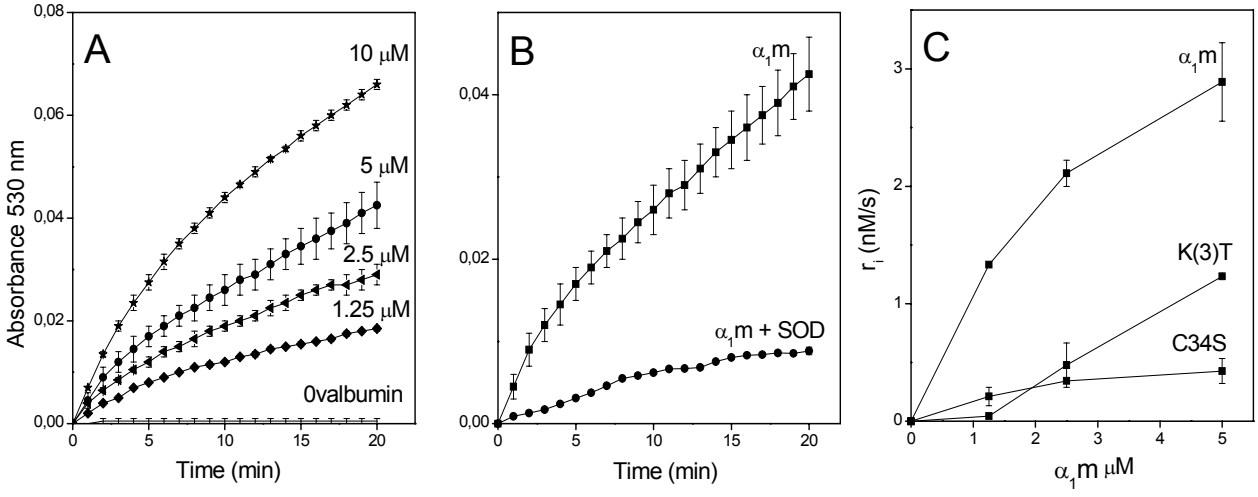
A
10 μM
5 μM
2.5 μM
1.25 μM
0valbumin
Absorbance 530 nm
Time (min)
B
α1m
α1m + SOD
Time (min)
C
α1m
K(3)T
C34S
ri (nM/s)
α1m μM

Figure 9

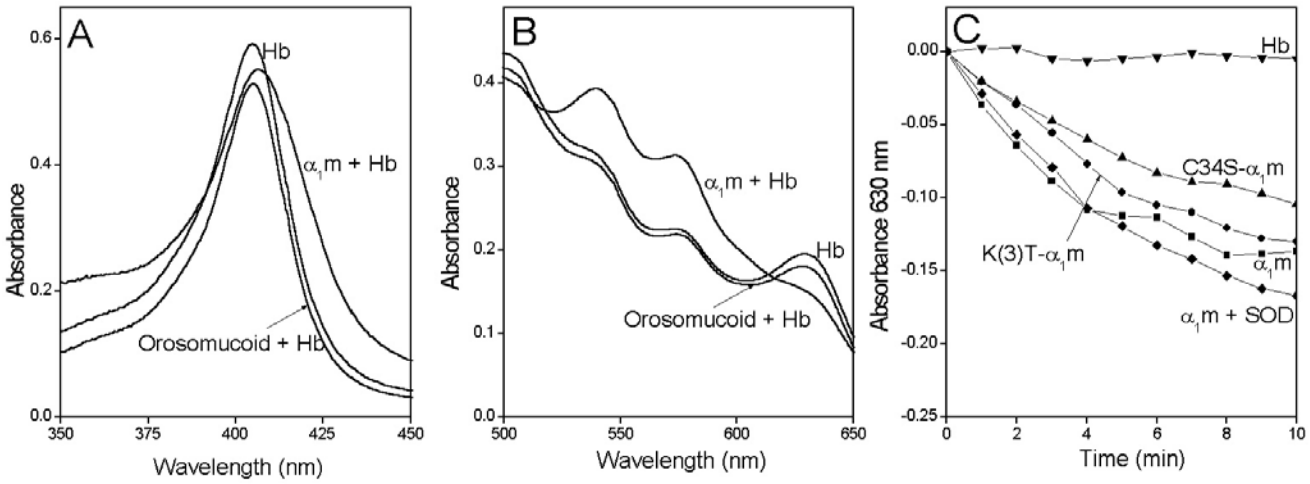
A
Hb
α1m + Hb
Orosomucoid + Hb
Absorbance
Wavelength (nm)
B
α1m + Hb
Hb
Orosomucoid + Hb
Absorbance
Wavelength (nm)
C
Hb
C34S-α1m
K(3)T-α1m
α1m
α1m + SOD
Absorbance 630 nm
Time (min)

Figure 10

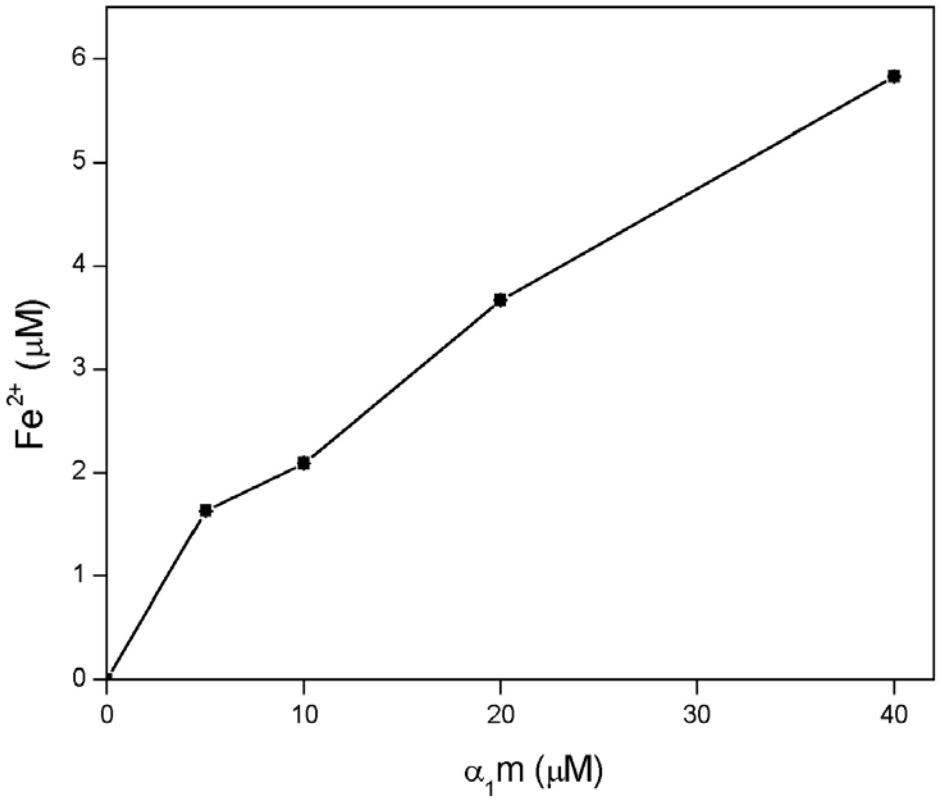

Figure 11

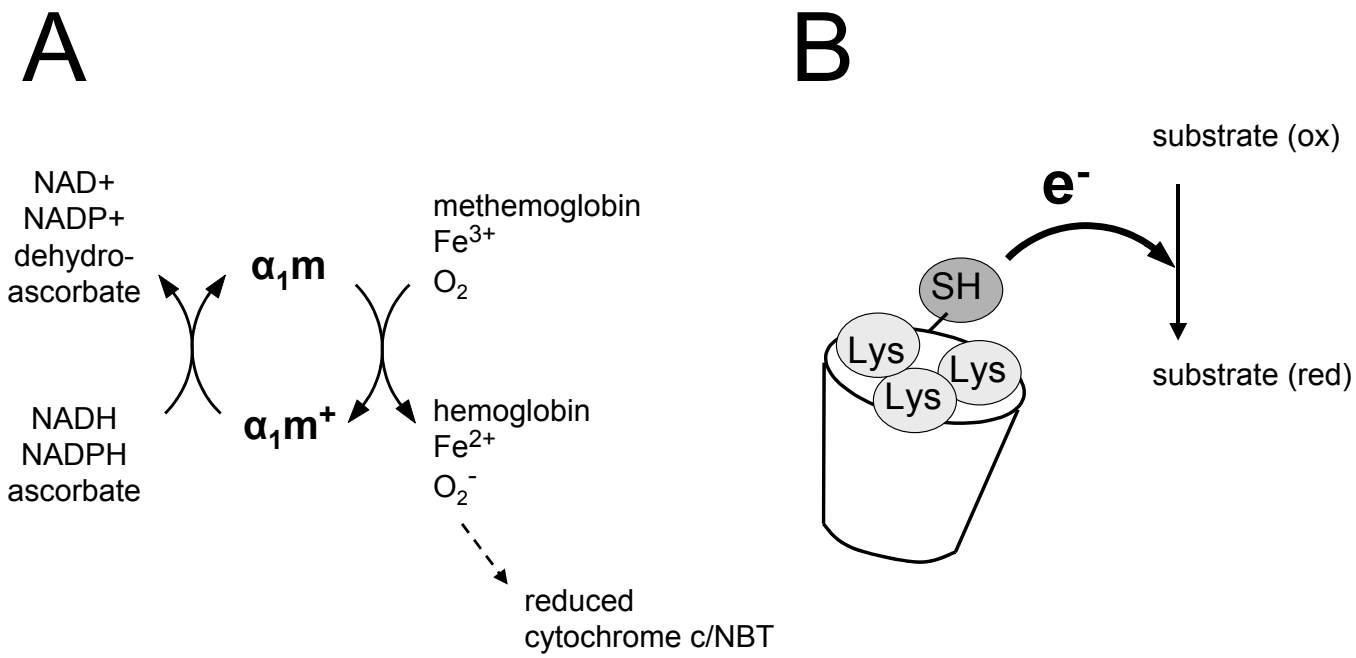
A
NAD+
NADP+
dehydro-
ascorbate
α1m
methemoglobin
Fe3+
O2
NADH
NADPH
ascorbate
α1m+
hemoglobin
Fe2+
O2-
reduced
cytochrome c/NBT
B
substrate (ox)
e-
SH
Lys
Lys
Lys
substrate (red)